

Intramolecular C–H and C–F Bond Oxygenation Mediated by a Putative Terminal Oxo Species in Tetranuclear Iron Complexes

Graham de Ruiter, Niklas B. Thompson, Michael K. Takase, and Theodor Agapie*

Division of Chemistry and Chemical Engineering, California Institute of Technology, Pasadena, California 91125, United States

S Supporting Information

ABSTRACT: Herein we report the intramolecular arene C–H and C–F bond oxygenation by tetranuclear iron complexes. Treatment of $[\text{LFe}_3(\text{PhPz})_3\text{OFe}][\text{OTf}]_2$ (**1**) or its fluorinated analog $[\text{LFe}_3(\text{F}_2\text{ArPz})_3\text{OFe}][\text{OTf}]_2$ (**5**) with iodosobenzene results in the regioselective hydroxylation of a bridging pyrazolate ligand, converting a C–H or C–F bond into a C–O bond. The observed reactivity suggests the formation of terminal and reactive Fe-oxo intermediates. With the possibility of intramolecular electron transfer within clusters in **1** and **5**, different reaction pathways (Fe^{IV}-oxo vs Fe^{III}-oxo) might be responsible for the observed arene hydroxylation.

Terminal metal-oxo species are proposed intermediates in a variety of biological transformations including water oxidation, dioxygen reduction, and C–H bond functionalization.¹ While the synthesis and characterization of complexes modeling enzyme active sites that display terminal metal-oxo moieties have seen remarkable development,² multinuclear analogs are significantly less studied.³ Except for synthetic dinuclear transition-metal complexes, accessing reactive terminal metal-oxo moieties on well-defined multinuclear iron complexes is rare.^{4,5} Nonetheless high-oxidation-state metal-oxo species on multimetallic scaffolds are desirable for systematic structure function studies in order to understand their reactivity.

We recently reported the rational synthesis of a family of tetranuclear iron clusters that are site-differentiated with an iron center in trigonal geometry and three metal centers six-coordinate.⁶ The site-differentiation allowed nitric oxide binding at the tripodal center and redox chemistry localized at the remaining sites, remotely tuning the degree of NO activation.⁶ Herein, we employ this platform to target terminal iron-oxo moieties on a metal cluster. Addition of oxygen atom-transfer reagents to the metal clusters leads to the regioselective conversion of ligand C–H and C–F bonds into C–O bonds, consistent with the formation of a terminal iron-oxo species as reactive intermediate. To the best of our knowledge, this is one of the very few examples suggesting the formation of highly reactive terminal oxo moieties on a multinuclear iron cluster.

High-oxidation-state iron-oxo complexes were targeted from the previously synthesized $[\text{LFe}_3(\text{PhPz})_3\text{OFe}][\text{OTf}]_2$ (**1**, Scheme 1; PhPz = 3-phenylpyrazolate).⁶ Treating **1** with iodosobenzene (PhIO; 1.1 equiv) resulted in significant changes in the ¹H NMR spectrum and is consistent with the formation of an asymmetric species (**2**; Figure S19). Analysis of

the reaction mixture by electrospray ionization mass spectrometry (ESI-MS) shows a shift of the peak for $[\text{LFe}_3(\text{PhPz})_3\text{OFe}]^{2+}$ ($m/z = 762.1$) to a peak consistent with $[\text{LFe}_3(\text{PhPz})_3\text{OFe}(\text{O})]^{2+}$ ($m/z = 769.6$), indicating the incorporation of an oxygen atom together with the loss of an H atom (Figures S34–S35). Moreover, with tetrabutylammonium periodate (ⁿBu₄NIO₄), similar results were obtained (Figure S22).

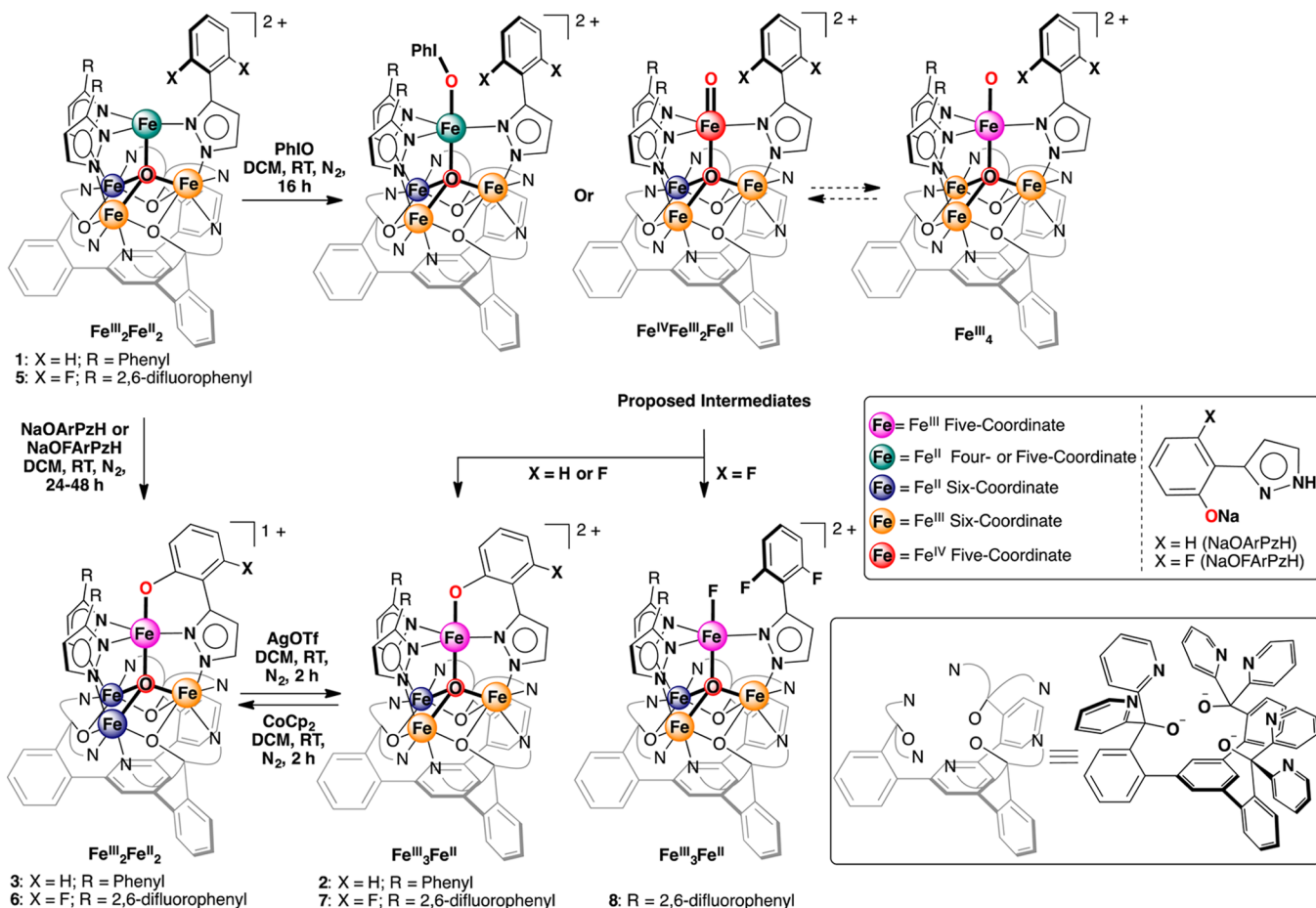
Single crystal X-ray diffraction (XRD) analysis of **2** revealed the regioselective hydroxylation of the bridging pyrazolate ligand (Figure 1). The coordination environment around the apical iron center (Fe4) is distorted trigonal bipyramidal ($\tau_5 = 0.72$),⁷ with the μ_4 -oxido (O1) and phenoxido (O40) in the axial positions and N14|N24|N34 spanning the equatorial plane. The apical iron center is connected to the Fe_{core} (Fe_{core} = Fe1–Fe3) through the μ_4 -oxido O1, resulting in a tetrahedral $[\text{Fe}_4(\mu_4\text{-O})]$ motif. In previously reported complexes, the Fe_{core}–O1 bond distances are characteristic of the presence of Fe^{II} or Fe^{III} centers.^{6,8} However, due to crystallographic disorder, we could not assign the iron oxidation states with certainty. Nevertheless, for Fe4, the Fe4–O1 distance of 1.931(4) Å is shorter compared to those in previously reported complexes **1** (1.971(2) Å) and $[\text{LFe}_3(\text{PhPz})_3\text{OFe}][\text{OTf}]_3$ (2.031(2) Å), suggesting a more oxidized iron center (Fe^{III}) at the apical position (Fe4). The iron oxidation states in **2** were assigned by using zero-field ⁵⁷Fe Mössbauer spectroscopy and by independent synthesis of **2** (*vide infra*). The Mössbauer spectrum of **2** (Figures 2 and S38) features four quadrupole doublets in a 1:1:1:1 ratio. The quadrupole doublet at $\delta = 1.17$ mm/s ($|\Delta E_Q| = 2.96$ mm/s) is consistent with a high-spin ferrous center in the triiron core (Figure 2; blue trace).⁹ The quadrupole doublets with identical isomer shifts of $\delta = 0.47$ mm/s and quadrupole splittings of $|\Delta E_Q| = 0.56$ and 0.99 mm/s, are indicative of the presence of two high-spin ferric ions (Figure 2; orange traces).⁹ The observed Mössbauer parameters (Table S4) are similar to our previously reported triiron-oxo/hydroxo clusters⁸ and to our, and other reported, complexes featuring a discrete $[\text{Fe}_4(\mu_4\text{-O})]$ core.^{6,8,10} Based on these parameters the oxidation state of the triiron core in **2** is thus assigned as $[\text{Fe}^{\text{II}}\text{Fe}^{\text{III}}_2]$.

The remaining quadrupole doublet at $\delta = 0.40$ mm/s ($|\Delta E_Q| = 1.72$ mm/s) is assigned to the apical iron Fe4, as a Fe^{III} metal center (Figure 2; purple trace).⁹ Such values are consistent with high-spin Fe^{III}.⁹ A detailed discussion on the assignment of the quadrupole doublets in the Mössbauer spectra is presented in

Received: November 22, 2015

Published: January 13, 2016

Scheme 1. Synthesis of Tetranuclear Iron Complexes



the Supporting Information. Further studies are required to determine the exact spin-states in complexes 2–8.

The assignment of the apical iron as a Fe^{III} metal center suggests an overall oxidation state in 2 as [LFe^{II}Fe^{III}₂(PhPz)₂(OArPz)OFe^{III}][OTf]₂. However, an assignment of [LFe^{II}Fe^{III}₂(PhPz)₂(HOArPz)OFe^{II}][OTf]₂ is also plausible, where the apical iron is Fe^{II} and the oxygenated ligand is a phenol rather than a phenoxide. In order to rule out any ambiguity, we independently synthesized 2 from 1. Treatment of 1 with NaOArPzH leads to complex 3 by protonolysis of a PhPz ligand. Oxidation of 3 with AgOTf provides 2 based on ¹H NMR spectroscopy (Scheme 1; Figure S21). XRD analysis of 3 shows that Fe_{core}–O1 bond distances of 2.154(3) Å (Fe1–O1), 2.119(3) Å (Fe2–O1), and 1.938(3) Å (Fe3–O1) are consistent with an assignment of a [Fe^{II}₂Fe^{III}] triiron core (Table S1; Figure S45). Based on charge balance with 1, from which 3 was synthesized, the apical iron Fe4 is a Fe^{III} metal center. The isomer shift and quadrupole splitting ($\delta = 0.46$ mm/s; $|\Delta E_Q| = 1.84$ mm/s) for the apical iron Fe4 (Figure S39, Table S4) is similar to 2 and supports the assignment of the apical iron center as Fe^{III}. Furthermore, the short Fe4–O1 (1.867(3) Å) and Fe4–O40 (1.911(4) Å) distances are in agreement to those found in complex 2 (Table S1) and are in line with other reported Fe(III)–phenoxide complexes.¹¹ Taking these data into account, the formal iron oxidation states are assigned as [LFe^{II}₂Fe^{III}(PhPz)₂(OArPz)OFe^{III}][OTf] (3) and [LFe^{II}Fe^{III}₂(PhPz)₂(OArPz)OFe^{III}][OTf]₂ (2). Thus, the isolated product 2 shows overall C–H bond oxygenation with formal loss of a hydrogen atom.

Similar hydroxylation pathways have been observed in other monometallic nonheme iron complexes, where Fe^{IV}-oxo moieties are the (proposed) reactive intermediates.^{11,12} The observed intramolecular hydroxylation in 1 thus hints at the formation of a high-valent Fe^{IV}-oxo as intermediate, although other reaction pathways cannot be excluded, including hydroxylation from a PhIO adduct (Scheme 1).¹³ Further studies might reveal more mechanistic details of this process. Nonetheless, the Fe-oxo species implicated here is unusual in that the tetrairon cluster, a multinuclear motif with four redox-active metal centers, supports it.

In order to prolong the lifetime of the putative Fe^{IV}-oxo species, by avoiding intramolecular C–H bond hydroxylation, we synthesized the fluorinated analog of 1; [LFe₃(F₂ArPz)₃OFe][OTf]₂ (5; F₂ArPz = 3-(2,6-difluorophenyl)pyrazolate, Figure S46). Treatment of 5 with PhIO (1.1 equiv) results in a mixture of at least two species: (i) [LFe₃(F₂ArPz)₂(FArPz)OFe(O)]²⁺ (7; *m/z* = 814.6) and (ii) [LFe₃(F₂ArPz)₃OFe(F)]²⁺ (8; *m/z* = 825.6), as judged by ESI-MS and ¹H NMR (Figures S26 and S36–S37). Using ⁿBu₄NIO₄ as an oxygen atom-transfer reagent resulted only in the formation of 7 (Figure S30). These data are consistent with incorporation of an oxygen atom with loss of a fluorine atom, suggesting C–F to C–O bond conversion (Scheme 1).

In order to establish the identity of species 7 and 8, they were synthesized independently (Scheme 1). Treating 5 with NaOFArPzH results in the formation of a new species, [LFe₃(F₂ArPz)₂(OFArPz)OFe][OTf] (6; Figure S28). Subsequent oxidation of 6 with silver triflate (AgOTf; 1.0 equiv)

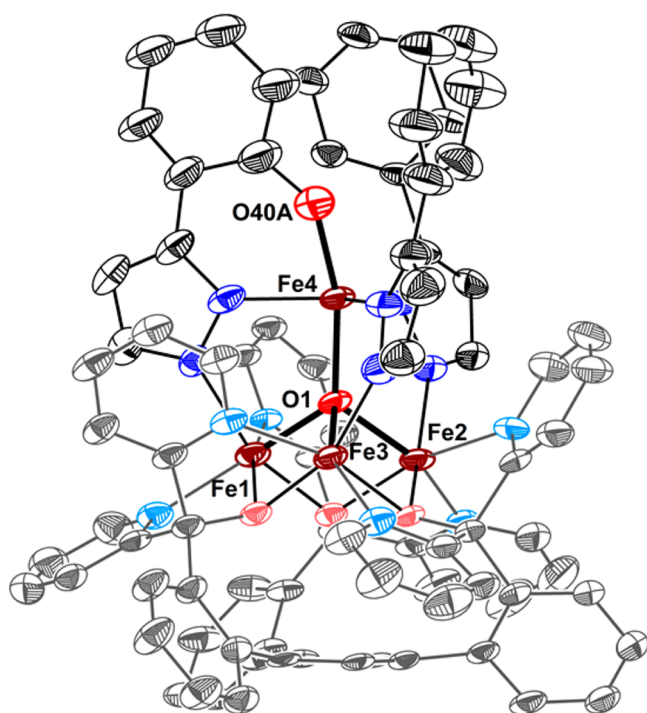


Figure 1. Crystal structure of $[\text{LFe}_3(\text{PhPz})_2(\text{OArPz})\text{OFe}][\text{OTf}]_2$ (**2**). Thermal ellipsoids are shown at the 50% probability level. Hydrogen atoms, outer sphere counter ions, and co-crystallized solvent molecules are not shown for clarity.

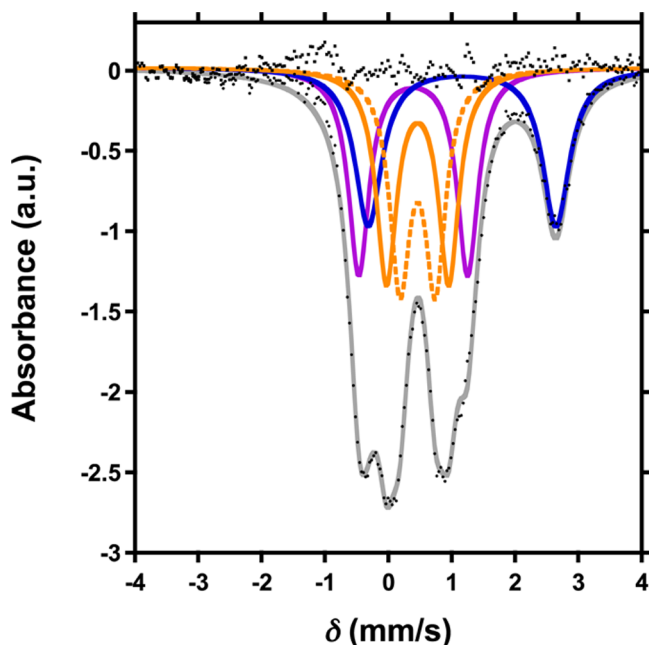


Figure 2. Zero-field ^{57}Fe Mössbauer spectra (80 K) of $[\text{LFe}_3(\text{PhPz})_2(\text{OArPz})\text{OFe}][\text{OTf}]_2$ (**2**).

produced a species with ^1H NMR characteristics identical to species **7** (Figures S27 and S29). The crystal structure of **7** (Figure 3A) is nearly identical to **2**. The coordination environment around the apical iron center is a distorted trigonal bipyramid ($\tau_5 = 0.89$).⁷ The $\text{Fe}_{\text{core}}\text{--O1}$ bond distances of 2.198(4) Å (Fe1–O1), 1.978(4) Å (Fe2–O1), and 1.986(4) Å (Fe3–O1) are consistent with an oxidation state of $[\text{Fe}^{\text{II}}\text{Fe}^{\text{III}}_2]$ for the triiron core. Similar to **2**, the apical iron is

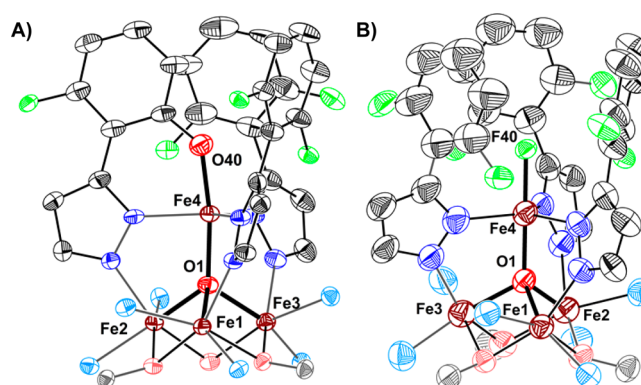


Figure 3. Crystal structure of (A) $[\text{LFe}_3(\text{F}_2\text{ArPz})_2(\text{OArPz})\text{OFe}][\text{OTf}]_2$ (**7**) and (B) $[\text{LFe}_3(\text{F}_2\text{ArPz})_3\text{OFe}(\text{F})][\text{OTf}]_2$ (**8**). Thermal ellipsoids are shown at the 50% probability level. Hydrogen atoms, parts of the ligand L, outer sphere counter ions, and co-crystallized solvent molecules are not shown for clarity.

assigned as Fe^{III} based on the short Fe4–O1 bond distance (1.914(3) Å, Table S1) and the zero-field ^{57}Fe Mössbauer parameters (Figure S42 and Table S4).^{6,8,10} The byproduct of C–F bond oxygenation (**8**) was independently synthesized from complex **5** and xenon difluoride (XeF_2 ; 1.0 equiv). Species **8** was identified as $[\text{LFe}^{\text{II}}\text{Fe}^{\text{III}}_2(\text{F}_2\text{ArPz})_3\text{Fe}^{\text{III}}(\text{F})][\text{OTf}]_2$ by XRD analysis (Figure 3B). The Mössbauer spectra and parameters resemble those reported for **2** and **7** (Figure S43 and Table S4). The independent synthesis of **7** and **8** demonstrates the regioselective conversion of the pyrazolate C–F bond into a C–O bond, by a putative Fe-oxo species. The overall reaction is balanced, with the oxygenated product losing fluoride and formally oxidizing by one electron the cluster that accepts the fluoride ligand.

While C–H bond hydroxylation has ample precedent with Fe-oxo species, C–F hydroxylation is very rare. This reactivity has been recently observed with a nonheme iron complex where treatment of $[\text{Fe}^{\text{II}}(\text{N}4\text{Py}^{2\text{PhF}_2})(\text{NCMe})][\text{BF}_4]_2$ with oxygen atom-transfer reagents resulted in intramolecular C–F bond hydroxylation.¹⁴ That reactivity resulted from a detectable Fe^{IV} -oxo intermediate. Recently, a copper facilitated C–F bond oxygenation was reported, proposed to involve a high-oxidation-state $\text{Cu}^{\text{III}}_2(\text{O})_2$ species.¹⁵ In both examples, the orientations of the C–F bond and the aromatic π -system were deemed important for the observed reactivity. Although we have not observed the proposed terminal Fe-oxo intermediate, such species are in line with precedent for both C–H and C–F bond functionalization.^{11,12,14} The present multinuclear clusters also present the distinct mechanistic possibility of internal electron transfer, leading to a Fe^{III} -oxo species, expected to be very basic.¹⁶ Recent studies have shown that the reactivity of such intermediates (Fe^{IV} -oxo vs Fe^{III} -oxo) can be very different.¹⁷ A Fe^{III} -oxo could undergo C–F activation via a nucleophilic attack, although typically high-oxidation-state metal-oxo species are proposed to perform arene hydroxylation via electrophilic mechanisms.^{11c,12,14,18} Additionally, the spin state of the Fe-oxo species, shown to influence reactivity, can be affected in the reported clusters by metal–metal interactions. Current efforts are directed toward elucidating the mechanism of C–H and C–F bond activation from **1** and **5**.

In summary, we have demonstrated the intramolecular oxygenation of C–H and C–F bonds upon treatment of tetranuclear iron complexes **1** and **5** with oxygen atom-transfer reagents. These processes suggest the involvement of a high-

oxidation-state Fe-oxo, which is rare on well-defined multi-nuclear scaffolds. The possibility of intramolecular electron transfer offers several potential mechanistic pathways for bond activation engendered by the presence of proximal spin- and redox-active metals.

■ ASSOCIATED CONTENT

■ Supporting Information

The Supporting Information is available free of charge on the ACS Publications website at DOI: 10.1021/jacs.5b12214.

Crystallographic data (CIF)

General considerations, physical methods, and synthetic procedures. Figures S1–S48, Tables S1–S4 (PDF)

■ AUTHOR INFORMATION

Corresponding Author

*agapie@caltech.edu

Notes

The authors declare no competing financial interest.

■ ACKNOWLEDGMENTS

This research was supported by the NIH (R01-GM102687A). T.A. is grateful for Sloan, Dreyfus, and Cottrell fellowships. T.A. and G.de R. are grateful for a Camille & Henry Dreyfus Environmental Chemistry Fellowship. We thank Lawrence M. Henling for assistance with crystallography.

■ REFERENCES

- (1) (a) Solomon, E. I.; Heppner, D. E.; Johnston, E. M.; Ginsbach, J. W.; Cirera, J.; Qayyum, M.; Kieber-Emmons, M. T.; Kjaergaard, C. H.; Hadt, R. G.; Tian, L. *Chem. Rev.* **2014**, *114*, 3659. (b) Yano, J.; Yachandra, V. *Chem. Rev.* **2014**, *114*, 4175. (c) Poulos, T. L. *Chem. Rev.* **2014**, *114*, 3919. (d) Tinberg, C. E.; Lippard, S. J. *Acc. Chem. Res.* **2011**, *44*, 280. (e) Costas, M.; Mehn, M. P.; Jensen, M. P.; Que, L. *Chem. Rev.* **2004**, *104*, 939. (f) Feig, A. L.; Lippard, S. J. *Chem. Rev.* **1994**, *94*, 759.
- (2) (a) Boaz, N. C.; Bell, S. R.; Groves, J. T. *J. Am. Chem. Soc.* **2015**, *137*, 2875. (b) Baglia, R. A.; Prokop-Prigge, K. A.; Neu, H. M.; Siegler, M. A.; Goldberg, D. P. *J. Am. Chem. Soc.* **2015**, *137*, 10874. (c) Taguchi, T.; Gupta, R.; Lassalle-Kaiser, B.; Boyce, D. W.; Yachandra, V. K.; Tolman, W. B.; Yano, J.; Hendrich, M. P.; Borovik, A. S. *J. Am. Chem. Soc.* **2012**, *134*, 1996. (d) Park, Y. J.; Ziller, J. W.; Borovik, A. S. *J. Am. Chem. Soc.* **2011**, *133*, 9258. (e) Lacy, D. C.; Gupta, R.; Stone, K. L.; Greaves, J.; Ziller, J. W.; Hendrich, M. P.; Borovik, A. S. *J. Am. Chem. Soc.* **2010**, *132*, 12188. (f) McGown, A. J.; Kerber, W. D.; Fujii, H.; Goldberg, D. P. *J. Am. Chem. Soc.* **2009**, *131*, 8040. (g) Rohde, J.-U.; In, J.-H.; Lim, M. H.; Brennessel, W. W.; Bukowski, M. R.; Stubna, A.; Münck, E.; Nam, W.; Que, L. *Science* **2003**, *299*, 1037. (h) MacBeth, C. E.; Golombek, A. P.; Young, V. G.; Yang, C.; Kuczera, K.; Hendrich, M. P.; Borovik, A. S. *Science* **2000**, *289*, 938. (i) Groves, J. T.; Haushalter, R. C.; Nakamura, M.; Nemo, T. E.; Evans, B. J. *J. Am. Chem. Soc.* **1981**, *103*, 2884. (j) Puri, M.; Que, L. *Acc. Chem. Res.* **2015**, *48*, 2443. (k) Nam, W. *Acc. Chem. Res.* **2015**, *48*, 2415. (l) Cook, S. A.; Borovik, A. S. *Acc. Chem. Res.* **2015**, *48*, 2407. (m) McDonald, A. R.; Que, L., Jr. *Coord. Chem. Rev.* **2013**, *257*, 414. (n) Hohenberger, J.; Ray, K.; Meyer, K. *Nat. Commun.* **2012**, *3*, 720. (o) Borovik, A. S. *Chem. Soc. Rev.* **2011**, *40*, 1870. (p) Que, L. *Acc. Chem. Res.* **2007**, *40*, 493. (q) Nam, W. *Acc. Chem. Res.* **2007**, *40*, 522.
- (3) (a) Khenkin, A. M.; Kumar, D.; Shaik, S.; Neumann, R. *J. Am. Chem. Soc.* **2006**, *128*, 15451. (b) de Visser, S. P.; Kumar, D.; Neumann, R.; Shaik, S. *Angew. Chem., Int. Ed.* **2004**, *43*, 5661.
- (4) (a) Stoian, S. A.; Xue, G.; Bominaar, E. L.; Que, L.; Münck, E. *J. Am. Chem. Soc.* **2014**, *136*, 1545. (b) Kodera, M.; Kawahara, Y.; Hitomi, Y.; Nomura, T.; Ogura, T.; Kobayashi, Y. *J. Am. Chem. Soc.* **2012**, *134*, 13236. (c) Do, L. H.; Xue, G.; Que, L.; Lippard, S. J. *Inorg. Chem.* **2012**, *51*, 2393. (d) Kudrik, E. V.; Afanasiev, P.; Alvarez, L. X.; Dubourdeaux, P.; Clémancey, M.; Latour, J.-M.; Blondin, G.; Bouchu, D.; Albrieux, F.; Nefedov, S. E.; Sorokin, A. B. *Nat. Chem.* **2012**, *4*, 1024. (e) Xue, G.; De Hont, R.; Münck, E.; Que, L. *Nat. Chem.* **2010**, *2*, 400. (f) Xue, G.; Fiedler, A. T.; Martinho, M.; Münck, E.; Que, L. *Proc. Natl. Acad. Sci. U. S. A.* **2008**, *105*, 20615.

(5) For some recent iron clusters studied for other applications, including their redox properties, catalysis, and small molecule reactivity, see: (a) Hernández Sánchez, R.; Zheng, S.-L.; Betley, T. A. *J. Am. Chem. Soc.* **2015**, *137*, 11126. (b) Nguyen, A. D.; Rail, M. D.; Shanmugam, M.; Fettinger, J. C.; Berben, L. A. *Inorg. Chem.* **2013**, *52*, 12847. (c) Lee, Y.; Sloane, F. T.; Blondin, G.; Abboud, K. A.; García-Serres, R.; Murray, L. J. *Angew. Chem., Int. Ed.* **2015**, *54*, 1499.

(6) de Ruiter, G.; Thompson, N. B.; Lionetti, D.; Agapie, T. *J. Am. Chem. Soc.* **2015**, *137*, 14094.

(7) Addison, A. W.; Rao, T. N.; Reedijk, J.; van Rijn, J.; Verschoor, G. C. *J. Chem. Soc., Dalton Trans.* **1984**, 1349.

(8) Herbert, D. E.; Lionetti, D.; Rittle, J.; Agapie, T. *J. Am. Chem. Soc.* **2013**, *135*, 19075.

(9) Gutlich, P.; Eckhard, B.; Trautwein, A. X. *Mössbauer Spectroscopy and Transition Metal Chemistry*; Springer: Berlin, 2011.

(10) (a) Sutradhar, M.; Carrella, L. M.; Rentschler, E. *Eur. J. Inorg. Chem.* **2012**, *2012*, 4273. (b) Murali, M.; Nayak, S.; Costa, J. S.; Ribas, J.; Mutikainen, I.; Turpeinen, U.; Clémancey, M.; Garcia-Serres, R.; Latour, J.-M.; Gamez, P.; Blondin, G.; Reedijk, J. *Inorg. Chem.* **2010**, *49*, 2427.

(11) (a) Mehn, M. P.; Fujisawa, K.; Hegg, E. L.; Que, L. *J. Am. Chem. Soc.* **2003**, *125*, 7828. (b) Harman, W. H.; Chang, C. J. *J. Am. Chem. Soc.* **2007**, *129*, 15128. (c) Sahu, S.; Widger, L. R.; Quesne, M. G.; de Visser, S. P.; Matsumura, H.; Moënné-Loccoz, P.; Siegler, M. A.; Goldberg, D. P. *J. Am. Chem. Soc.* **2013**, *135*, 10590.

(12) (a) Cook, S. A.; Ziller, J. W.; Borovik, A. S. *Inorg. Chem.* **2014**, *53*, 11029. (b) Bigi, J. P.; Harman, W. H.; Lassalle-Kaiser, B.; Robles, D. M.; Stich, T. A.; Yano, J.; Britt, R. D.; Chang, C. J. *J. Am. Chem. Soc.* **2012**, *134*, 1536. (c) England, J.; Guo, Y.; Farquhar, E. R.; Young, V. G., Jr.; Münck, E.; Que, L., Jr. *J. Am. Chem. Soc.* **2010**, *132*, 8635. (d) England, J.; Martinho, M.; Farquhar, E. R.; Frisch, J. R.; Bominaar, E. L.; Münck, E.; Que, L. *Angew. Chem., Int. Ed.* **2009**, *48*, 3622. (e) Nielsen, A.; Larsen, F. B.; Bond, A. D.; McKenzie, C. J. *Angew. Chem., Int. Ed.* **2006**, *45*, 1602. (f) Jensen, M. P.; Lange, S. J.; Mehn, M. P.; Que, E. L.; Que, L. *J. Am. Chem. Soc.* **2003**, *125*, 2113. (g) Mekmouche, Y.; Ménage, S.; Toia-Duboc, C.; Fontecave, M.; Galey, J.-B.; Lebrun, C.; Pécaut, J. *Angew. Chem., Int. Ed.* **2001**, *40*, 949. (h) Hegg, E. L.; Ho, R. Y. N.; Que, L. *J. Am. Chem. Soc.* **1999**, *121*, 1972.

(13) (a) Collman, J. P.; Chien, A. S.; Eberspacher, T. A.; Brauman, J. I. *J. Am. Chem. Soc.* **2000**, *122*, 11098. (b) Hong, S.; Wang, B.; Seo, M. S.; Lee, Y.-M.; Kim, M. J.; Kim, H. R.; Ogura, T.; Garcia-Serres, R.; Clémancey, M.; Latour, J.-M.; Nam, W. *Angew. Chem., Int. Ed.* **2014**, *53*, 6388.

(14) Sahu, S.; Quesne, M. G.; Davies, C. G.; Dürr, M.; Ivanović-Burmazović, I.; Siegler, M. A.; Jameson, G. N. L.; de Visser, S. P.; Goldberg, D. P. *J. Am. Chem. Soc.* **2014**, *136*, 13542.

(15) Serrano-Plana, J.; Garcia-Bosch, I.; Miyake, R.; Costas, M.; Company, A. *Angew. Chem., Int. Ed.* **2014**, *53*, 9608.

(16) Gupta, R.; Borovik, A. S. *J. Am. Chem. Soc.* **2003**, *125*, 13234.

(17) Usharani, D.; Lacy, D. C.; Borovik, A. S.; Shaik, S. *J. Am. Chem. Soc.* **2013**, *135*, 17090.

(18) (a) Ansari, A.; Kaushik, A.; Rajaraman, G. *J. Am. Chem. Soc.* **2013**, *135*, 4235. (b) de Visser, S. P.; Oh, K.; Han, A.-R.; Nam, W. *Inorg. Chem.* **2007**, *46*, 4632.